ORIGINAL ARTICLE

Encapsulation of epigallocatechin-3-gallate into albumin nanoparticles improves pharmacokinetic and bioavailability in rat model

Nithya Ramesh[1] · Abul Kalam Azad Mandal[1]

Abstract

In the present study, we fabricated epigallocatechin-3-gallate (EGCG) loaded albumin nanoparticles (Alb-NP-EGCG) to enhance bioavailability and improve pharmacokinetic parameters of EGCG. The physicochemical properties of the Alb-NP-EGCG were studied using scanning electron microscopy, differential scanning calorimetry, powder X-ray diffraction and in vitro release studies. Characterization of Alb-NP-EGCG indicated the formation of spherical nanoparticles with no drug and excipient interaction. Alb-NP-EGCG showed a high drug loading capacity of 92%. Further, in vitro study showed a sustained release of EGCG from Alb-NP-EGCG over a period of 48 h. Mathematical modeling and release kinetics indicated that the Alb-NP-EGCG followed zero order kinetic and EGCG was released via fickian diffusion method. In vivo bioavailability and distribution of Alb-NP-EGCG showed an enhanced plasma concentration of EGCG with 1.5 fold increase along with prolonged $T_{1/2}$ of 15.6 h in the system when compared with the free EGCG. All this study demonstrated the fabrication of EGCG loaded albumin nanoparticles which favored the slow and sustained release of EGCG with improved pharmacokinetics and bioavailability thereby prolonging the action of EGCG. Additional acute and sub-acute toxicity test of the Alb-NP-EGCG demonstrated the safety of the Alb-NP-EGCG. Therefore, the Alb-NP-EGCG could be a promising drug delivery system for EGCG.

Keywords Albumin nanoparticles · EGCG · Bioavailability · Toxicity study · Sustained release

Introduction

Green tea consumption has been associated with multiple health benefits, particularly its active derivative epigallocatechin-3-gallate (EGCG) has shown to modulate many pharmacological properties in cancer (Lambert and Yang 2003; Thangapazham et al. 2007; Rahmani et al. 2015), inflammatory (Tominari et al. 2015; Leichsenring et al. 2016) and cardiovascular diseases (Eng et al. 2018). Further, EGCG has shown the potential to inhibit reactive oxygen species and apoptosis, chelate metals, and modulate multiple signaling pathways (Hechler et al. 2006; Karatas et al. 2009; Schroeder et al. 2009). As an antioxidant agent, EGCG is more potent than vitamin C and E (Rice-Evans et al. 1995; Weinreb et al. 2004).

On oral administration of EGCG, the rate of ingestion is < 5% in human and only 1% in the rat (Nakagawa et al. 1997; Yang et al. 1998). Lower penetration of EGCG across the intestinal layer reduces its bioavailability and pharmacological action (Zhang et al. 2004; Tian et al. 2006; Li et al. 2014b). Additionally, it also has poor stability, low solubility, and is affected by factors like light, temperature, gastrointestinal enzymes, pH of the stomach, interaction with food, metabolism, and insufficient absorption time, which together further limit the beneficial attributes of EGCG (Pool et al. 2012).

To overcome these problems, nanotechnology can be considered as a promising oral drug delivery system. Nanoparticles have shown to improve solubility, stability, and provide a better rate of absorption in many cases (Krishna Sailaja and Vineela 2014; Li et al. 2014b). They are mainly employed for their ability to control the release of drug and provide a site-specific delivery. Additionally, it is possible

✉ Abul Kalam Azad Mandal
akamandal@rediffmail.com

1 School of Bio Sciences and Technology, Vellore Institute of Technology, Vellore, TN 632014, India

to modulate the size of nanoparticles during preparation. Nanoparticles can be either from natural or synthetic compounds; for instance, albumin, gelatin, chitosan, and alginate fall under natural compounds, while poly(lactic acid), poly(lactic-*co*-glycolic acid), and poly-L-lysine fall under synthetic compounds. These nanocarriers either covalently bind, entrap, or adsorb the drug and enhance its therapeutic potential, stability, bioavailability, and solubility (Lockman et al. 2002; Barbu et al. 2009; Cupaioli et al. 2014). For instance, the use of EGCG encapsulated in PLA–PEG nanoparticles have shown high antioxidant and metal chelation potential when compared to its free form (Singh et al. 2018a), EGCG and doxycycline encapsulated poly(lactic-*co*-glycolic acid) (PLGA) nanoparticles have shown to effectively reduce oxidative stress (Singh et al. 2015), EGCG encapsulated PLGA sheets have also potential as anti-adhesion barriers (Lee et al. 2014), EGCG loaded PLA–PEG nanoparticles when used in vitro have shown an inhibitory effect on Al(III) induced $A\beta_{42}$ fibrillation (Singh et al. 2018b) and at in vivo it has reversed Al(III) induced cognitive impairment and Alzheimer's disease pathology (Singh et al. 2018a). Therefore, nanoparticles show potential to be used as a delivery system for EGCG.

The current study employs albumin, a natural compound, as a drug carrier, mainly because it is biodegradable, biocompatible, and non-toxic in nature and is capable of acting as a transport plasma protein (Elsadek and Kratz 2012; Ferrado et al. 2018). The carboxylic and amino functional groups present on the surface of albumin molecules bind to the drug by means of covalent attachment or site targeting agent (e.g. folic acid conjugate, transferrin) (Tang et al. 2011; Ulbrich et al. 2011). Many anticancer drugs have been incorporated into albumin nanoparticles because of their high binding affinity toward albumin (Dreis et al. 2007; Kratz 2008). Active and passive pathways are the major transport mechanism through which albumin can penetrate into cancer cells (Kratz 2008; Fu et al. 2009). In 2005, Food and Drug Administration (FDA) has approved the first albumin based nanoparticle (paclitaxel loaded in albumin nanoparticles) formulation which has shown enhanced solubility of the drug used in cancer therapy (Gradishar et al. 2005; Desai et al. 2006). Curcumin and paclitaxel co-loaded in albumin nanoparticles as a carrier have shown to improve the anticancer efficacy in pancreatic cancer when compared with free form of the drug (Kim et al. 2016), albumin nanoparticles loaded with rhodamine B have shown a controlled release of the drug over a period of 150 h and in vivo distribution have shown that rhodamine diffuse near eustachian tube and inner ear of guinea pig which can be used in the treatment of ear disorder (Yu et al. 2014). Various studies have shown that albumin as a carrier has improved the efficacy of the drug in vitro as well as in vivo (Merodioa et al. 2000; Ulbrich et al. 2011; Woods et al. 2015; Kumar et al.

2016). The most common method of preparing albumin nanoparticles is desolvation of albumin with solvent followed by cross-linking with glutaraldehyde (Gallo et al. 1984). This method helps to improve the particle size and polydispersity index (PDI) by varying parameters such as the concentration of albumin, pH value, and a cross-linking agent (Yedomon et al. 2013).

Therefore, the main objective of the present study was to synthesize and characterize the albumin nanoparticles and test their bioavailability and toxicity in a rat model. We hypothesize that the prepared albumin nanoparticles will improve the absorption rate of EGCG by preventing its degradation, and increase bioavailability.

Materials and methods

Materials

Bovine serum albumin (BSA), glutaraldehyde, and epigallocatechin-3-gallate (EGCG) were purchased from Sigma Aldrich Co, USA. HPLC grade acetic acid (glacial) and acetonitrile were obtained from Himedia, India.

Preparation and purification of albumin nanoparticles

Albumin nanoparticles were prepared by desolvation technique with slight modification (Weber et al. 2000). About 200 mg of BSA was dissolved in 2 ml distilled water followed by dropwise (at a flow rate of 1 ml min^{-1}) addition of 8 ml ethanol under continuous stirring. An opalescent solution was formed indicating the formation of the nanoparticles. To prepare EGCG loaded albumin nanoparticles (Alb-NP-EGCG), 10 mg of EGCG was added along with 8% glutaraldehyde (235 μl) as a crosslinking agent in order to increase the stability of nanoparticles. The mixture was kept overnight to ensure cross-linking of amino acid moieties with the drug molecule under constant stirring. Purification of the prepared albumin nanoparticles was done by centrifugation for 15 min at 10,000 rpm. The process was repeated with three cycles by re-dispersing the sample with the same volume of distilled water.

Characterization of nanoparticles

Physicochemical properties

High resolution—scanning electron microscopy (HR-SEM, FEI Quanta FEG 200) analysis was carried out to determine the structural morphology and particle sizes of the prepared albumin nanoparticles. Albumin nanoparticles (Alb-NP-EGCG) were coated on a carbon button and gold sputtering

was done to take images. Particle size and zeta potential of unloaded albumin nanoparticles (Alb-NP-UL) and albumin nanoparticles loaded with EGCG (Alb-NP-EGCG) were measured using Horiba SZ-100 (dynamic light scattering). Particles were dispersed in water before measurement. The functional groups' characterization of free EGCG, Alb-NP-UL, and Alb-NP-EGCG was studied using Fourier transform infrared spectroscopy (FT-IR spectroscopy, Siemens 578564). The lyophilized nanoparticles were subjected to FTIR spectroscopy measurement in diffuse reflectance mode at a resolution of 4 cm^{-1} in KBr pellets. To better understand the physical properties of the prepared nanoparticles, X-ray diffraction (X-ray diffraction instrument, D8 Advance, BRUKER, Germany) and differential scanning calorimetry (DSC Universal V4.5A Instrument) were performed for free EGCG and Alb-NP-EGCG. For DSC analysis, lyophilized samples were sealed in a standard aluminum pan and purged with constant nitrogen, set at a flow rate of 10 °C min^{-1} and the heat flow was recorded from 35 to 350 °C. Circular dichroism (CD) (Jasco, J-715 CD) was performed for BSA, Alb-NP-UL, and Alb-NP-EGCG to determine the conformational change in the protein structure. The measurements were carried out in a quartz cuvette with 1 cm path length at a wavelength range of 200–290 nm with a bandwidth of 1 nm.

Encapsulation efficiency and in vitro drug release

HPLC method was followed to determine the concentration of EGCG encapsulated into Alb-NP-EGCG. The albumin nanoparticles were centrifuged at 10,000 rpm for 15 min and EGCG was quantified in the supernatant. Encapsulation efficiency (EE) was calculated using the following formula (Patel et al. 2013)

$$EE\ (\%) = \{(\text{Total amount of initial EGCG}$$
$$- \text{Amount of EGCG in the supernatant})/$$
$$\text{Total amount of EGCG})\} \times 100.$$

The amount of EGCG released from Alb-NP-EGCG up to 48 h in phosphate buffer solution (PBS) at pH 1.2 and pH 7.4 were studied using dialysis bag diffusion technique. Briefly, the Alb-NP-EGCG was loaded in a dialysis membrane (12,000–14,000 Da) and placed in a beaker containing PBS as a release medium under constant stirring at room temperature. At the specific time interval, 1 ml of the sample was collected and replenished with an equal volume of release medium. The collected samples were analyzed by HPLC method to determine the concentration of EGCG released from the albumin nanoparticles over a period of 48 h.

$$\text{Release}\ (\%) = \{(\text{Amount of EGCG released at time } t/$$
$$\text{Total amount of EGCG encapsulated})\} \times 100.$$

The amount of EGCG was estimated in the HPLC system connected to a UV detector. HPLC chromatogram was obtained using Phenomenex Luna™ C18 column and a mobile phase containing a mixture of 87.5% v/v of acetic acid (1% v/v) and 12.5% v/v of acetonitrile. The mobile phase and samples were filtered through a 0.22 μ Millipore membrane filter before analysis. The mobile phase was pumped at a flow rate of 1 ml min^{-1} with isocratic conditions at 25 °C and UV detection at 280 nm was used (Dube et al. 2011).

Mathematical modeling

To better understand the release kinetics mechanism of Alb-NP-EGCG, the data obtained from in vitro release study at pH 1.2 and 7.4 were fitted into mathematical kinetic models (Dash et al. 2010). The best fit model and the release mechanism were determined using the correlation coefficient (R^2) value and the release exponent (n) value, respectively.

In vivo pharmacokinetic study

Dosing of rat and sample collection

Two groups of Wistar albino rats weighing around 200–250 g were used to study the pharmacokinetics after a single oral administration of free EGCG and Alb-NP-EGCG at a dose of 10 mg kg^{-1} (Leichsenring et al. 2016; Stringer et al. 2017). Rats were sacrificed at a time interval of 1, 2, 3, 4, 6, 8, and 24 h after oral drug administration and the blood and tissue samples (liver, kidney, spleen, and brain) were collected. Three rats were sacrificed at each given time point. The experiment was approved by the institutional animal ethical committee.

About 1 ml of the blood sample was treated with EDTA, centrifuged at 3000 rpm for 10 min, and the supernatant was stored at -80 °C. Tissue samples of liver, spleen, kidney, and brain were collected, weighed, washed twice with ice-cold PBS and stored at − 80 °C. For extraction of EGCG, the tissue samples were homogenized with sodium phosphate buffer (pH 6.5). The homogenates were centrifuged and the supernatants were used for further analysis. For determination of EGCG in plasma and tissue samples, the supernatants were incubated with 10 μl of 50 M K$_2$HPO$_4$ at 37 °C for 45 min. To each of these mixtures, 500 μl of ethyl acetate was added, mixed, centrifuged at 10,000 rpm for 5 min, and the supernatants were collected. The process of ethyl acetate extraction was repeated. Both the supernatants were taken together and kept in a nitrogen evaporator to remove ethyl acetate (Chen et al. 1997). The residues were dissolved in 100 μl of mobile phase and analyzed to determine the amount of EGCG present at each time point by HPLC
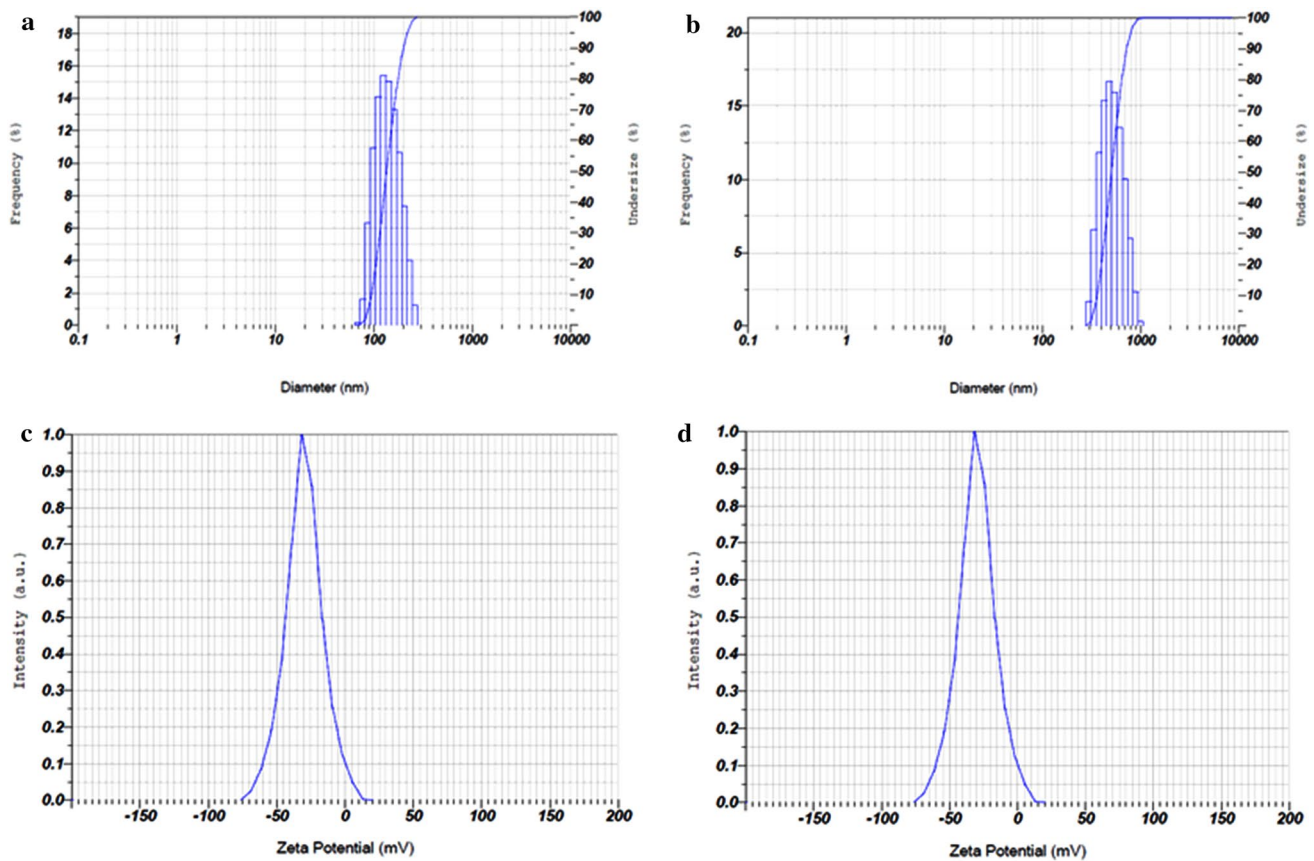
Fig. 1 Particle size analysis image of **a** Alb-NP-UL and **b** Alb-NP-EGCG and zeta potential analysis of **c** Alb-NP-UL and **d** Alb-NP-EGCG

method as previously described. The level of EGCG in the tissues was expressed as µg/g of wet weight.

Toxicokinetic study

The study protocol for toxicokinetics study was approved by the institutional animal ethical committee.

Acute toxicity study

The male Wistar albino rats were orally administrated with a single dose (1000, 1500, 2000 mg kg^{-1} of body weight) of free EGCG and Alb-NP-EGCG and monitored for 24 h for clinical signs of toxicity or mortality (Chinedu et al. 2013).

Sub-acute toxicity

The Wistar albino rats were divided into three groups, each group containing three rats. Rats of group I (control) were given with normal saline, rats of group II were daily treated with free EGCG at the dose of 10 mg kg^{-1} body weight for a period of 28 days, and rats of group III were daily treated with Alb-NP-EGCG at the dose of 10 mg kg^{-1} body weight for a period of 28 days. The rats were inspected for any clinical signs of morbidity and mortality. Further, the change in body weight and food intake rate was also observed.

At the end of 28 days of treatment, the rats were sacrificed, blood and organ samples (liver, Spleen, and kidney) were collected for histopathological studies.

Histopathological study

Liver, spleen, and kidney samples of rats treated with free EGCG and Alb-NP-EGCG were collected, washed, and fixed with 10% formalin solution. The paraffin blocks were prepared for the tissue, thin sections (5 µm) were cut in a microtome, stained with hematoxylin and eosin and viewed under light microscopy.
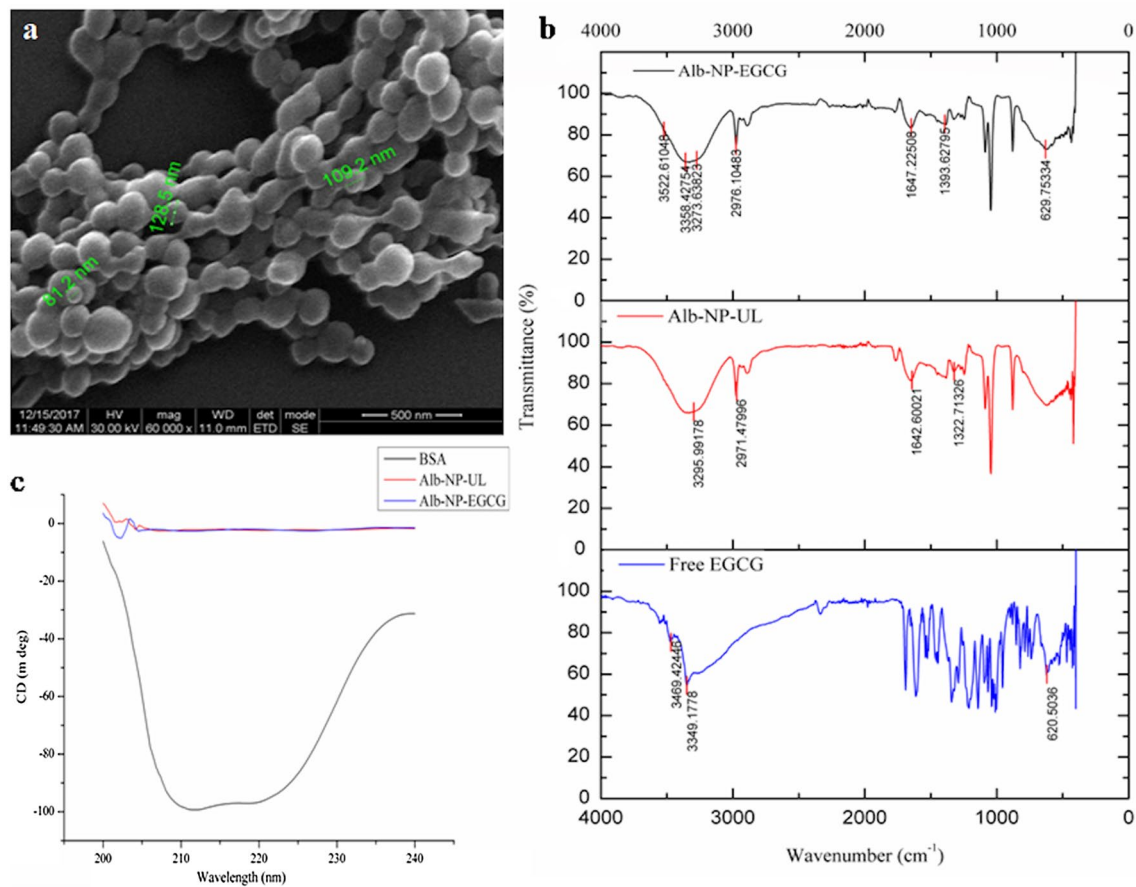
Fig. 2 Physicochemical properties of nanoparticles. **a** SEM image of Alb-NP-EGCG; **b** the FT-IR spectrum of free EGCG, Alb-NP-UL, and Alb-NP-EGCG; **c** circular dichroism analysis of BSA, Alb-NP-UL, and Alb-NP-EGCG
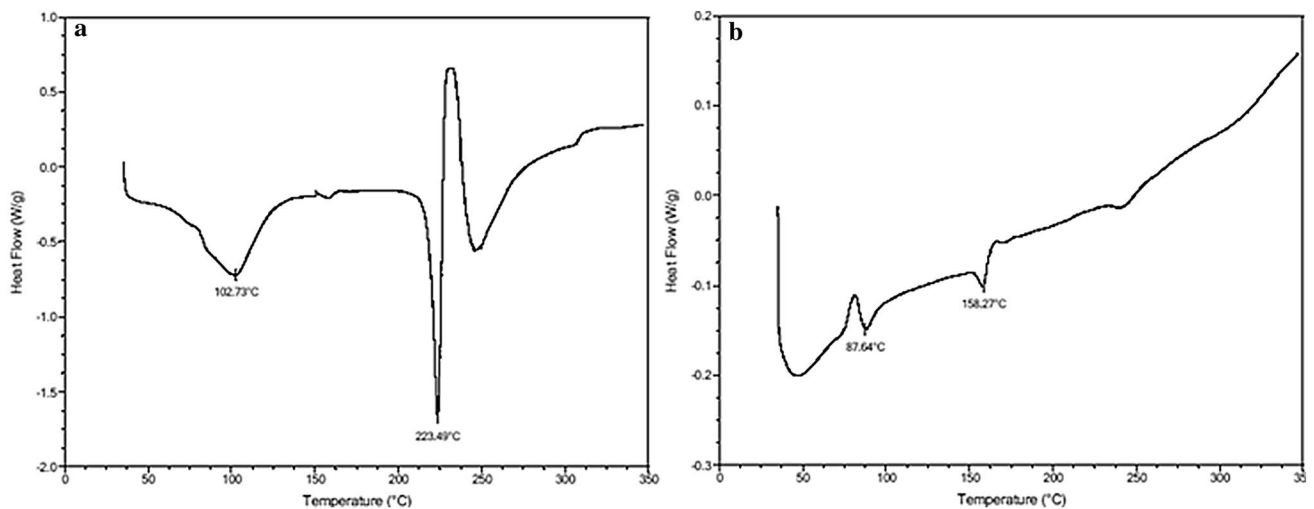

Fig. 3 Differential scanning calorimetry analysis of **a** free EGCG and **b** Alb-NP-EGCG
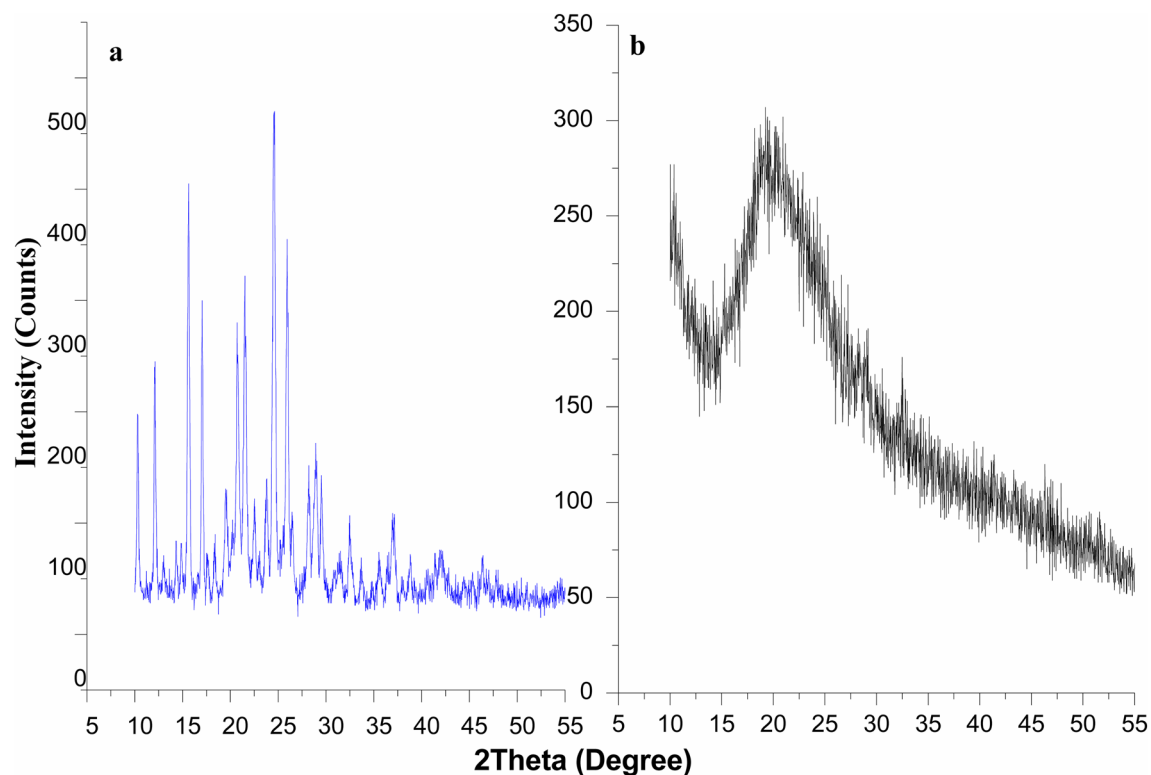
Fig. 4 X-ray diffraction (X-RD) analysis of **a** free EGCG and **b** Alb-NP-EGCG

Results and discussion

Characterization of nanoparticles

Physiochemical properties

The size (hydrodynamic diameter) of the prepared unloaded albumin nanoparticles (Alb-NP-UL) and EGCG loaded albumin nanoparticles (Alb-NP-EGCG) was recorded as 292.6 ± 11.87 nm and 325.6 ± 6.7 nm with an average polydispersity index (PDI) of 0.308 ± 0.02 and 0.675 ± 0.1, respectively (Fig. 1a, b). The Alb-NP-UL and Alb-NP-EGCG have zeta potential values of -18.55 ± 0.07 mV and -29.9 ± 0 mV, respectively (Fig. 1c, d). Nanoparticles with an average size of around 300 nm exhibited enhanced membrane permeability and retention (EPR) effect (Bae et al. 2011; Saneja et al. 2017). The greater value of zeta potential represents the high stability of the prepared nanoparticles through prevention of particle aggregation (Freitas and Müller 1998; Bhushan et al. 2015; Kumari et al. 2018).

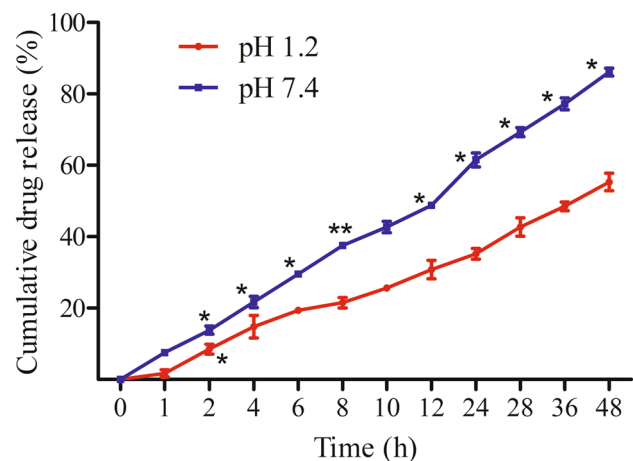The study of surface morphology and particle size of the prepared nanoparticles in SEM (Fig. 2a) showed

Fig. 5 In vitro release study of Alb-NP-EGCG at pH 7.4 and pH 1.2. Mean followed by the symbol (*) at each time interval are significantly different at $P < 0.001$(**), $P < 0.05$(*) according to t test

predominantly spherical shape along with a few oval shapes of the Alb-NP-EGCG with the size of around 150 nm.

The compatibility of EGCG with the components of the albumin nanoparticles was determined using FTIR (Fig. 2b). The characteristic peaks of free EGCG at 3348.42 cm^{-1} and 1689.64 cm^{-1} indicated the aromatic O–H group and C=O group, respectively, that links the trihydroxybenzoate group and chroman group at 1523.76 cm^{-1} for a C–C stretch in the aromatic ring. The spectrum of Alb-NP-UL showed characteristic peaks at 3296.35 cm^{-1}, 2976.16 cm^{-1}, 1641.4 cm^{-1}, and 1323.17 cm^{-1} representing the N–H stretching (amide A), NH_3^+ free ion stretching (amide B), C=O stretching (amide I) and CH_2 group bending, respectively. The spectra of Alb-NP-EGCG showed the characteristic peaks of Alb-NP-UL and EGCG indicating the compatibility of the components and did not interact chemically. Peaks present in a similar region of free EGCG and bovine albumin serum have been previously reported by others (Radhakrishnan et al. 2016; Bronze-Uhle et al. 2017).

Circular dichroism (CD)

Circular dichroism (CD) analysis was used to analyze the conformational change in the protein structure after loading the drug. CD analysis was performed for BSA, Alb-NP-UL, and Alb-NP-EGCG. After the formation of albumin nanoparticles, change in the protein structure of alpha-helical content was observed. BSA exhibited a negative band at 210 and 222 nm (Fig. 2c) in CD analysis, which is a distinguishing feature of high alpha-helical content (Pant et al. 2014). There was a decrease in an alpha-helical content after the formation of Alb-NP-UL and Alb-NP-EGCG with an increase in the negative bands at 210 and 220 nm indicating a change in the structural conformation of the protein after the formation of the nanoparticles. The CD analysis showed clear structural changes in alpha-helical rich protein in both Alb-NP-UL and Alb-NP-EGCG.

Differential scanning calorimetry

The DSC analysis was performed to determine the existing form of the drug encapsulated in the nanoparticles. The amorphous nature of the drug results in better absorption, improved pharmacokinetic, and solubility (Qi et al. 2011). DSC analysis of EGCG showed an endothermic melting peak at 223.47 °C, indicating its crystalline nature, which is consistent with the previous research (Radhakrishnan et al. 2016). However, in Alb-NP-EGCG, the characteristic peak of EGCG was disappeared and it showed an endothermic peak at 158.27 °C. The shift in the melting curve can be explained by a smaller particle size resulting in high surface energy (Suresh et al. 2007; Vivek et al. 2007). Less energy is required to melt the disordered crystalline form or amorphous state when compared with the crystalline form of the drug (Nayak et al. 2010) and thus indicating its amorphous nature after encapsulation into the nanoparticles (Fig. 3a, b). The amorphous nature of the Alb-NP-EGCG is also corroborated by our XRD data (Fig. 4d).

Powder X-ray diffractometry

The powder-XRD analysis was performed to determine the physical characterization of the drug and formulation. The XRD pattern of pure EGCG exhibited defined peaks at 2θ—angles 15.62, 17.05, 21.50, 24.60, and 25.92 indicating its crystalline nature (Fig. 4a). While Alb-NP-EGCG did not show any characteristic crystalline peaks of EGCG at 2θ—angles 15.62, 17.05, 21.50, 24.60, and 25.92 due to the amorphous nature of the formulation suggesting complete encapsulation of EGCG into albumin nanoparticles (Fig. 4b). The intensity of EGCG peaks was also decreased in the nano-formulation. The reduction in peak intensity suggested a decrease in the crystallinity of EGCG. The amorphous state found in the ALB-NP-EGCG is due to the mechanism of functional group cross-linking of a protein molecule with the hydrogen bonding of drug (Sanoj Rejinold et al. 2011). The change in the nature of lipid and drug plays a major role in the release mechanism of the drug from

Table 1 Release kinetic of EGCG from albumin nanoparticle loaded EGCG in pH 1.2 and pH 7.4

Kinetic model	Correlation co-efficient, R^2		Kinetic constant (K) and Release exponent (n)	
	pH 1.2	pH 7.4	pH 1.2	pH 7.4
Zero order	0.988	0.996	$k_0 = 0.2880$	$k_0 = 0.448$
First order	0.962	0.911	$k_1 = 0.0002$	$k_1 = 0.00005$
Higuchi model	0.971	0.995	$k_H = 15.45$	$k_H = 24.06$
Hixson–Crowell model	0.974	0.953	$k_{HC} = 0.00071$	$k_{HC} = 0.00019$
Korsmeyer–Peppas model	0.968	0.917	$n = 0.157$ Fickian diffusion	$n = 0.095$ Fickian diffusion

Table 2 Pharmacokinetic parameter of free EGCG and Alb-NP-EGCG after oral administration to rats in plasma and various organs

Parameters	Plasma		Brain		Liver		Kidney		Spleen	
	EGCG	Alb-NP-EGCG	EGCG	Alb-NP-EGCG	EGCG	Alb-NP-EGCG	EGCG	Alb-NP-EGCG	EGCG	Alb-NP-EGCG
V_d (ml)	47.8 ± 1.7	32.2 ± 1.3***	88.6 ± 12.7	113 ± 13.2	271 ± 33.9	37.1 ± 1.2***	106 ± 16	67.9 ± 3.3*	96.94 ± 8.5	41.0 ± 1.03***
C_o (μg ml^{-1})	41.8 ± 1.4	77.6 ± 3.3***	22.8 ± 3.5	22.2 ± 2.5	7.4 ± 0.9	67.3 ± 2.2***	19 ± 3.04	36.8 ± 1.7***	20.7 ± 1.8	60.8 ± 1.5***
Ke (h^{-1})	0.05 ± 0.005	0.04 ± 0.003*	0.07 ± 0.01	0.06 ± 0.003	0.05 ± 0.01	0.06 ± 0.006	0.03 ± 0.01	0.09 ± 0.01**	0.13 ± 0.01	0.01 ± 0.001***
AUC (mg h l^{-1})	536.8 ± 14.0	1048 ± 11.46***	254.8 ± 82	1637.9 ± 64***	104.7 ± 4.5	1107 ± 20.6***	332.7 ± 28.7	378.8 ± 17.01	163.3 ± 28.2	1803.4 ± 47.4***
$T_{1/2}$ (h)	12.2 ± 1.2	15.6 ± 1.2*	9.02 ± 1.5	10.6 ± 0.5	12.1 ± 3.3	10.8 ± 1.07	20.6 ± 11	7.4 ± 1.1	5.3 ± 0.7	65 ± 8.6***
C_{max} (μg ml^{-1})	53.1 ± 7.5	136 ± 4.8***	26.5 ± 3.9	131.8 ± 4.5***	11.42 ± 0.9	264 ± 3.9***	30.1 ± 2.3	58.54 ± 3.05***	63.3 ± 11.4	122.2 ± 2.1***
T_{max} (h)	1.6 ± 0.2	2 ± 0*	3.3 ± 0.5	4 ± 0	4.6 ± 1.1	4 ± 0	6 ± 0	3 ± 0	3 ± 0	8 ± 0
Cl (ml h^{-1})	0.002 ± 0.0001	0.001 ± 0.0001***	0.007 ± 0.002	0.007 ± 0.001	0.015 ± 0.002	0.002 ± 0.0001***	0.004 ± 0.001	0.006 ± 0.001	0.01 ± 0.002	0.0004 ± 0.0006**

Data are represented as mean ± SD ($n = 3$)

Level of significant between the means at $P < 0.0001$(***), $P < 0.001$(**), $P < 0.05$(*) are denoted by the repetition of the symbol (*)

the nanoparticles (Dudhipala and Veerabrahma 2015). The change of crystalline to amorphous form as evidenced by our data from DSC and X-RD analyses also indicated successful encapsulation of EGCG into albumin nanoparticles. Studies on albumin nanoparticles loaded with 5-methylmellein also showed similar results in X-RD and DSC data indicating successful encapsulation of drug into nanoparticles (Arora et al. 2017).

Encapsulation efficiency and In vitro release study

The encapsulation efficiency of EGCG from Alb-NP-EGCG was found to be $92 \pm 0.6\%$. In vitro release study was performed for Alb-NP-EGCG in pH 1.2 and pH 7.4 of the release medium (PBS) (Fig. 5). Release of EGCG from Alb-NP-EGCG in gastric pH 1.2 was performed to better understand the stability of nanoparticles in the gastric pH. In pH 1.2, after 24 h also only $35.2 \pm 0.2\%$ of EGCG was release and we observed $56 \pm 0.8\%$ of drug release at 48 h indicating the slow and sustained release of drug from the nanoparticles in acidic medium. During the initial first hour in pH 7.4, only $7.5 \pm 0.7\%$ of EGCG was released and about $50 \pm 1.4\%$ of EGCG was released from nanoparticles at 12 h and at the end of 48 h, around $86 \pm 1.07\%$ of EGCG was released. This pattern of release indicated sustained release of the drug without any burst release. The sustained release of EGCG could be due to the encapsulation of EGCG into albumin nanoparticles and thus Alb-NP-EGCG could have better therapeutic value with prolonged circulation (Zhao et al. 2010). Sustained release of other drugs from albumin nanoparticles have been reported in the previous studies also (Yu et al. 2014; Syame et al. 2018).

Mathematical modeling

Our Alb-NP-EGCG formulation showed a good linear correlation with zero order kinetics in both pH 1.2 and pH 7.4, which mainly applies to a pharmaceutical formulation for prolonged action (Costa and Lobos 2001; Dash et al. 2010; Ravi and Mandal 2015). The drug release mechanism for Alb-NP-EGCG ($n = 0.157$ and $n = 0.095$ for pH 1.2 and pH 7.4, respectively) followed the Fickian diffusion controlled process (Table 1).

Pharmacokinetic study

The plasma concentration of EGCG in rats administrated with a single dose of free ECGC and Alb-NP-EGCG was determined and the pharmacokinetic parameters were calculated (Table 2). The HPLC chromatogram of EGCG and plasma samples are presented in Fig. 6. Single oral administration of free EGCG and Alb-NP-EGCG showed maximum
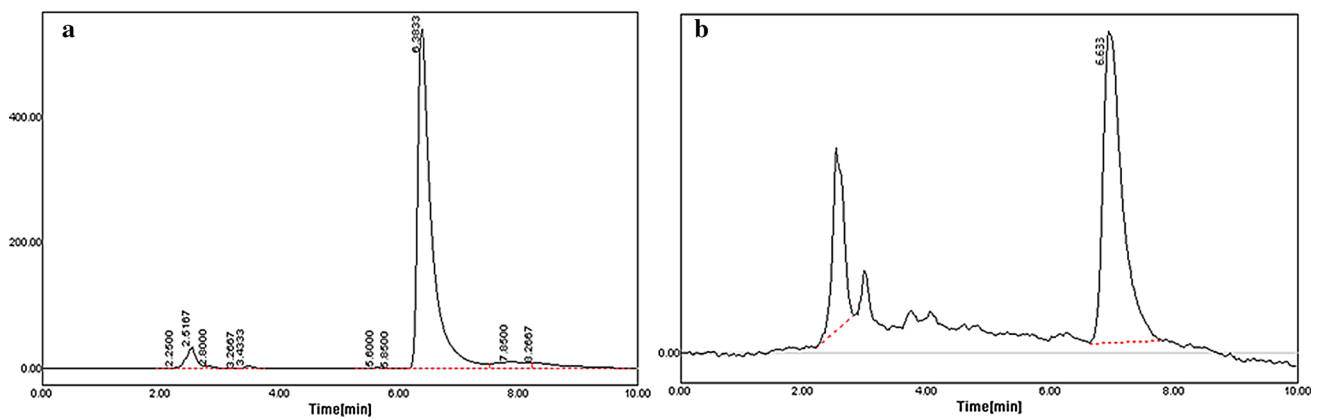
Fig. 6 HPLC chromatogram of **a** standard EGCG spiked with blank plasma and **b** plasma sample obtained from rats after oral administration of EGCG

drug concentration in plasma as 53.1 ± 7.5 µg ml^{-1} at 1.6 h and 136 ± 4.8 µg ml^{-1} at 2 h, respectively, which resulted in increased C_{max} of EGCG after encapsulation as presented in Fig. 7. There was a 1.5 fold increase in the concentration of EGCG released from Alb-NP-EGCG, which suggests the protection of EGCG from chemical degradation in the gastrointestinal tract. Alb-NP-EGCG showed a significant increase in plasma exposure (AUC: 1048 ± 11.46 mg h l^{-1}) compared to the free EGCG (AUC: 536.8 ± 14 mg h l^{-1}). This resulted in one fold increase in plasma exposure with Alb-NP-EGCG. The rate of clearance (Cl (ml h^{-1})) of EGCG released from Alb-NP-EGCG (0.001 ± 0.001 ml h^{-1}) was slower than that of free EGCG (0.002 ± 0.0001 ml h^{-1}). The pharmacokinetic parameters of Alb-NP-EGCG showed a significant increase of EGCG in plasma exposure (AUC) with a reduced clearance rate when compared with free EGCG indicated higher bioavailability of EGCG. There was a significant improvement in other pharmacokinetic parameters such as $T_{1/2}$ (h) and T_{max} (h) in Alb-NP-EGCG when
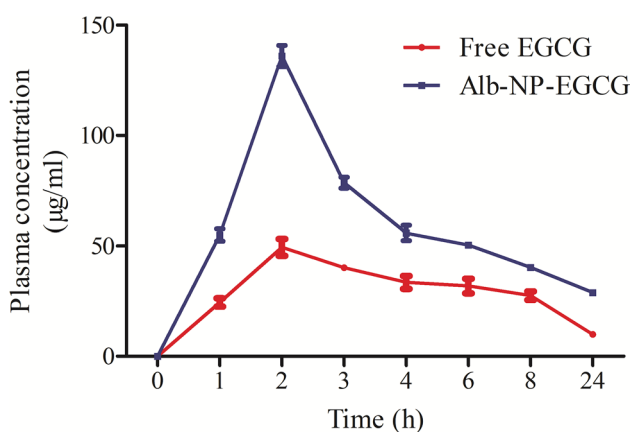
compared with free EGCG. Thus, encapsulation of EGCG into albumin nanoparticles improved the bioavailability of EGCG by prolonging drug retention time and also favored the slow and sustained release of EGCG with enhanced pharmacokinetics and bioavailability.

Distribution of EGCG and pharmacokinetic parameters in different organs were also studied after oral administration of free EGCG and Alb-NP-EGCG to rats at a dose of 10 mg/kg/body weight (Table 2). The mean concentration vs. time for free EGCG and EGCG released from Alb-NP-EGCG in organs are presented in Fig. 8. The concentration of EGCG in all the tissue samples of Alb-NP-EGCG administered rats were significantly increased when compared to free EGCG administration. The concentration of EGCG was higher in the liver, spleen, and brain samples of Alb-NP-EGCG administered rats than in free EGCG administered rats which may be due to the ability of albumin nanoparticles to cross the membrane through passive targeting pathway (Yang et al. 2007). Nanoparticles are absorbed by enterocytes and gut-associated lymphoid tissue (GALT) which mediates the transport between the systemic circulation and the drug release in the blood. Bioavailability of albumin nanoparticles can be improved by this uptake mechanism and also by avoiding the hepatic first-pass metabolism (Italia et al. 2007; Kumar et al. 2011). The significant increase in AUC value of EGCG released from Alb-NP-EGCG was seen in brain (1637 ± 64 mg h l^{-1}), liver (1107 ± 20 mg h l^{-1}), kidney (378 ± 17 mg h l^{-1}), and in spleen (1803 ± 47 mg h l^{-1}) when compared with the free EGCG.

The significant increase in the AUC level of EGCG released from Alb-NP-EGCG in all the organs may be due to the slow and sustained release of EGCG from the nanoparticles, the change in the absorption and elimination rate of EGCG as well as a slower rate of clearance when compared with the free EGCG. Similar studies have been reported in mice following oral administration of polymeric nanoparticles (Drummond
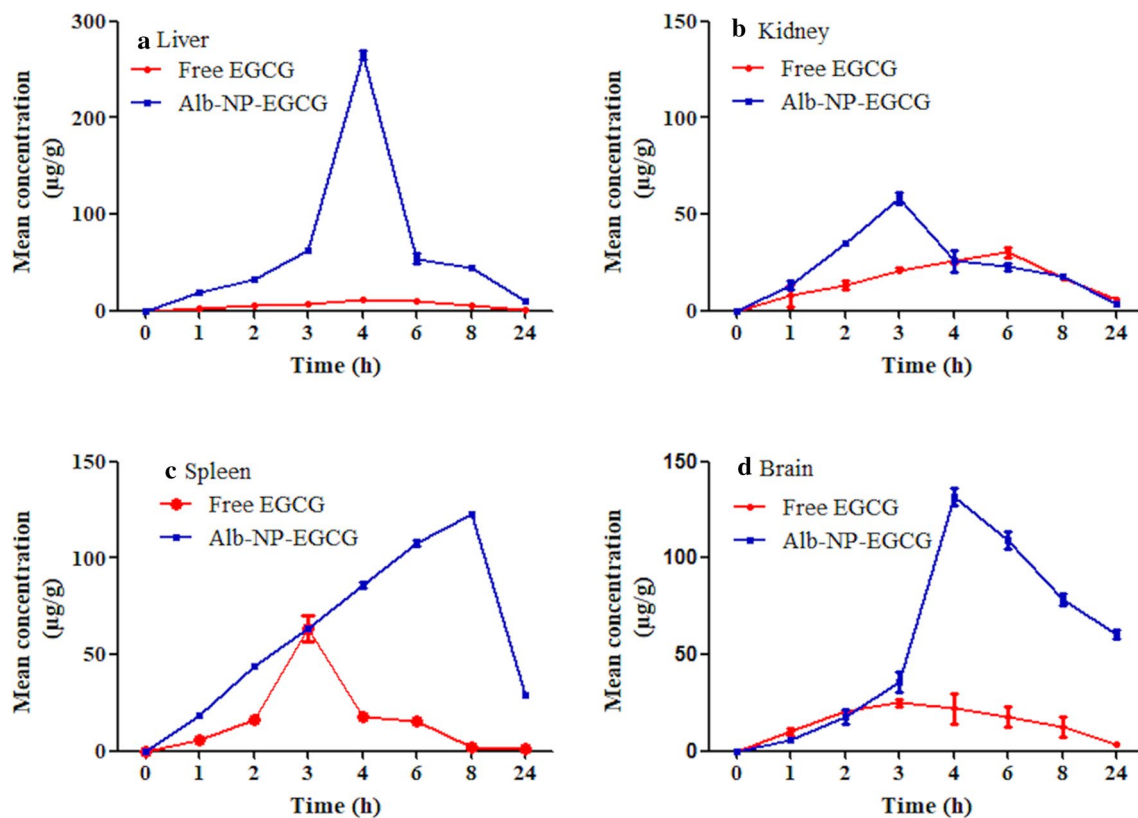

Fig. 7 The mean plasma concentration of free EGCG and Alb-NP-EGCG after oral administration to rats at a dose of 10 mg/kg

Fig. 8 Mean concentration of EGCG distributed in the organs after administration of free EGCG and Alb-NP-EGCG to rats. **a** Liver, **b** kidney, **c** spleen, and **d** Brain

et al. 2009; Kalaria et al. 2009). Studies on galactosylated bovine serum albumin loaded oridonin (Li et al. 2014a), and tea polyphenol-loaded gelatin nanoparticles (Kulandaivelu and Mandal 2017) also showed similar results of an increased rate of absorption with a decreased rate of clearance when compared to the free drug. Similar studies have been conducted in albumin nanoparticles loaded with docetaxel and quercetin after i.v. the administration showed a significant increase in AUC and $T_{1/2}$ when compared with the free drug (Desale et al. 2018). Studies on curcumin loaded albumin nanoparticles and bufalin loaded albumin nanoparticles also showed similar results (Jithan et al. 2011; Zhang et al. 2017). In the present study, Alb-NP-EGCG also showed an increase in plasma concentration, AUC, higher retention time when compared with the free EGCG. Alb-NP-EGCG exhibited sustained release of drug and improved bioavailability at in vivo studies.

Toxicokinetic study

Acute and sub-acute toxicity

Acute toxicity analysis of free EGCG and Alb-NP-EGCG treated with different concentrations showed no mortality of rats in any of the groups. Treated rats did not exhibit any

abnormal change in behavior or clinical sign of toxicity. Therefore, the Alb-NP-EGCG dose equivalent to 2000 mg kg^{-1} body weight (single administration) was indicated to be safe and non-toxic. Sub-acute toxicity study for free EGCG and Alb-NP-EGCG did not show mortality in rats. The study also showed that the Alb-NP-EGCG was non-ntoxic to rats and did not show any significant reduction in body weight with the prolonged oral administration.

Histopathology study

The histopathological analysis of control (group I), free EGCG (group II) and Alb-NP-EGCG (group III) treated rats were shown in Fig. 9. In group II, the liver samples showed no abnormal pathological change in the hepatocytes, portal triads when compared with that of group I, showing the liver sample with normal parenchyma cells and central vein. The rats of group III showed mild periportal inflammation and few congested sinusoids cell in the liver samples. Spleen tissue did not show any pathological change in the group II and III when compared with the group I. Spleen tissue was seen with normal white pulp with intervening red pulp in all the groups. In group III, the kidney tissues showed a normal architecture with mild congestion of the peritubular blood vessels whereas,
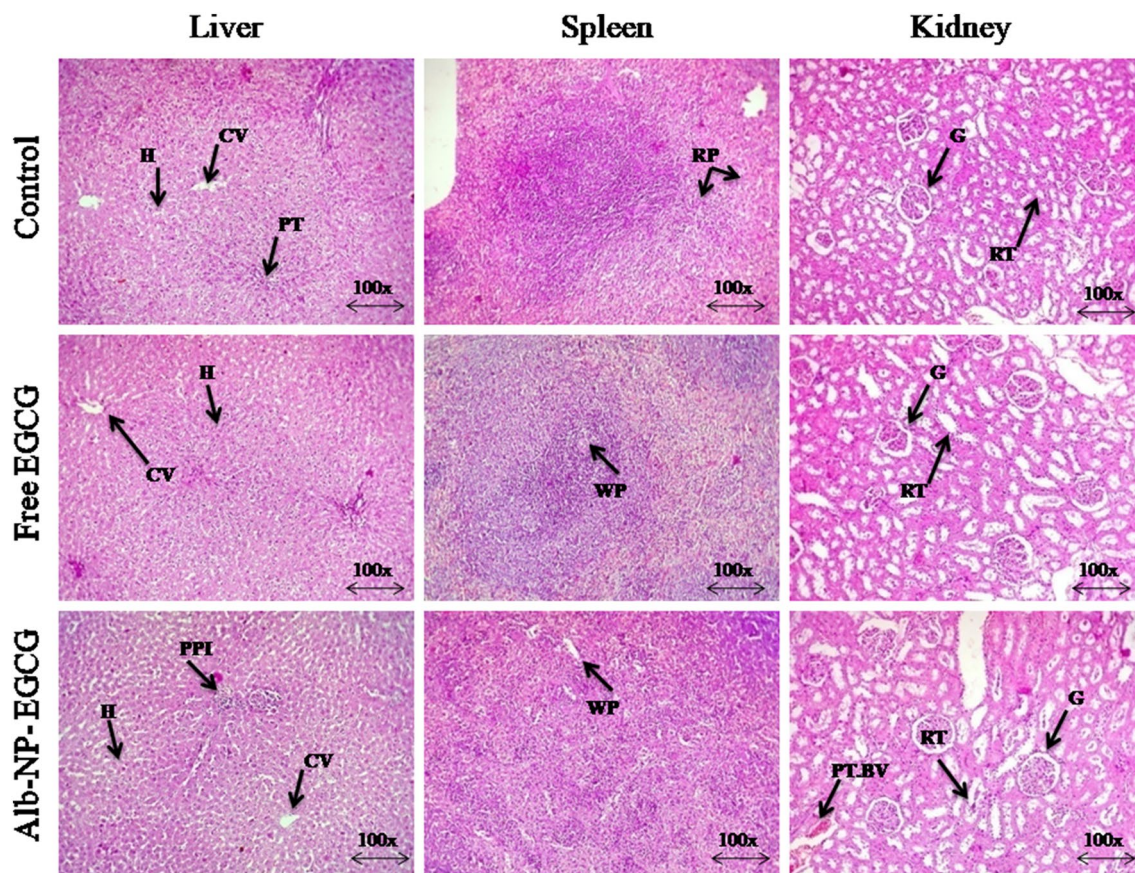
Fig. 9 Representative histopathological images of liver, spleen, and kidney after 28 days treatment of free EGCG and Alb-NP-EGCG. *H* hepatocytes, *CV* central vein, *PT* portal triads, *WP* white pulp, *RP* red pulp, *PPI* periportal inflammation, *RT* renal tubular, *G* glomerular, *PTBV* peritubular blood vessels

no abnormal changes in glomerulus and tubules in the kidney tissue were observed in group II. Similarly, studies on albumin nanoparticles loaded with docetaxel also showed a minimal hepatoxicity when compared with the free drug (Desale et al. 2018). Other drugs loaded into albumin nanoparticles were also found to be safe and effective (Zhang et al. 2017; Casa et al. 2018).

Conclusions

Albumin nanoparticles loaded with EGCG was successfully prepared by using desolvation method. We obtained an average particle size of 300 nm with a high encapsulation efficiency of EGCG. In vitro release study showed a sustained release of drug from the nanoparticles and zero-order release kinetic and EGCG release mechanism as fickian diffusion method. Incorporation of EGCG into nanoparticles was confirmed by DSC, XRD studies. In vivo pharmacokinetics studies showed a significant increase in the plasma concentration, greater AUC value and a prolonged drug residence time in the systemic circulation in case of Alb-NP-EGCG than the free EGCG. Acute and sub-acute toxicity study confirmed the safety of the prepared albumin nanoparticles loaded with EGCG. The histopathological analysis of albumin nanoparticles showed a slight inflammation in the liver sample. Thus the prepared albumin nanoparticles loaded with EGCG enhance the bioavailability, solubility, and improved therapeutic action and can act as an alternative drug delivery system for EGCG.

Author contributions AKAM was responsible for the concept and design of this study. NR performed all the experiments and compiled the results. NR and AKAM analyzed the data and drafted the manuscript. AKAM performed the final critical revision of the manuscript. All authors have read and approved the final manuscript.

Compliance with ethical standards

Conflict of interest The authors declare no conflict of interest.

References

Arora D, Kumar A, Gupta P et al (2017) Preparation, characterization and cytotoxic evaluation of bovine serum albumin nanoparticles encapsulating 5-methylmellein: a secondary metabolite isolated from Xylaria psidii. Bioorg Med Chem Lett 27:5126–5130. https://doi.org/10.1016/j.bmcl.2017.10.064

Bae KH, Chung HJ, Park TG (2011) Nanomaterials for cancer therapy and imaging. Mol Cells 31:295–302. https://doi.org/10.1007/s10059-011-0051-5

Barbu E, Molnàr É, Tsibouklis J, Górecki DC (2009) The potential for nanoparticle-based drug delivery to the brain: overcoming the blood–brain barrier. Expert Opin Drug Deliv 6:553–566. https://doi.org/10.1517/17425240902939143

Bhushan B, Dubey P, Kumar SU et al (2015) Bionanotherapeutics: niclosamide encapsulated albumin nanoparticles as a novel drug delivery system for cancer therapy. RSC Adv 5:12078–12086. https://doi.org/10.1039/c4ra15233f

Bronze-Uhle ES, Costa BC, Ximenes VF, Lisboa-Filho PN (2017) Synthetic nanoparticles of bovine serum albumin with entrapped salicylic acid. Nanotechnol Sci Appl 10:11–21. https://doi.org/10.2147/NSA.S117018

Casa DM, Scariot DB, Khalil NM et al (2018) Bovine serum albumin nanoparticles containing amphotericin B were effective in treating murine cutaneous leishmaniasis and reduced the drug toxicity. Exp Parasitol. https://doi.org/10.1016/j.exppara.2018.07.003

Chen L, Lee M, Li HE et al (1997) Absorption, distribution, elimination of tea polyphenols in rats. Drug Metab Dispos 25:1045–1050

Chinedu E, Arome D, Ameh FS (2013) A new method for determining acute toxicity in animal models. Toxicol Int 20:224–226. https://doi.org/10.4103/0971-6580.121674

Costa P, Lobo JMS (2001) Modelling and comparison of dissolution profiles. Eur J Pharm Sci 13:123–133. https://doi.org/10.1016/S0928-0987(01)00095-1

Cupaioli FA, Zucca FA, Boraschi D, Zecca L (2014) Engineered nanoparticles. How brain friendly is this new guest? Prog Neurobiol 119–120:20–38. https://doi.org/10.1016/j.pneurobio.2014.05.002

Dash S, Murthy PN, Nath L, Chowdhury P (2010) Kinetic modeling on drug release from controlled drug delivery systems. Acta Pol Pharm 67:217–223. https://doi.org/10.1016/S0928-0987(01)00095-1

Desai N, Trieu V, Yao Z et al (2006) Increased antitumor activity, intratumor paclitaxel concentrations, and endothelial cell transport of cremophor-free, albumin-bound paclitaxel, ABI-007, compared with cremophor-based paclitaxel. Clin Cancer Res 12:1317–1324. https://doi.org/10.1158/1078-0432.CCR-05-1634

Desale JP, Swami R, Kushwah V et al (2018) Chemosensitizer and docetaxel-loaded albumin nanoparticle: overcoming drug resistance and improving therapeutic efficacy. Nanomedicine 13:2759-2776. https://doi.org/10.2217/nnm-2018-0206

Dreis S, Rothweiler F, Michaelis M et al (2007) Preparation, characterisation and maintenance of drug efficacy of doxorubicin-loaded human serum albumin (HSA) nanoparticles. Int J Pharm 341:207–214. https://doi.org/10.1016/j.ijpharm.2007.03.036

Drummond DC, Noble CO, Guo Z et al (2009) Improved pharmacokinetics and efficacy of a highly stable nanoliposomal vinorelbine. J Pharmacol Exp Ther 328:321–330. https://doi.org/10.1124/jpet.108.141200

Dube A, Nicolazzo JA, Larson I (2011) Assessment of plasma concentrations of (À)-epigallocatechin gallate in mice following administration of a dose reflecting consumption of a standard green tea beverage. Food Chem 128:7–13. https://doi.org/10.1016/j.foodchem.2011.02.038

Dudhipala N, Veerabrahma K (2015) Pharmacokinetic and pharmacodynamic studies of nisoldipine-loaded solid lipid nanoparticles developed by central composite design. Drug Dev Ind Pharm 41:1968–1977. https://doi.org/10.3109/03639045.2015.1024685

Elsadek B, Kratz F (2012) Impact of albumin on drug delivery—new applications on the horizon. J Control Release 157:4–28. https://doi.org/10.1016/j.jconrel.2011.09.069

Eng QY, Thanikachalam PV, Ramamurthy S (2018) Molecular understanding of Epigallocatechin gallate (EGCG) in cardiovascular and metabolic diseases. J Ethnopharmacol 210:296–310. https://doi.org/10.1016/j.jep.2017.08.035

Ferrado JB, Perez AA, Visentini FF et al (2018) Formation and characterization of self-assembled bovine serum albumin nanoparticles as chrysin delivery systems. Colloids Surf B Biointerfaces 173:43–51. https://doi.org/10.1016/j.colsurfb.2018.09.046

Freitas C, Müller RH (1998) Effect of light and temperature on zeta potential and physical stability in solid lipid nanoparticle (SLN®) dispersions. Int J Pharm 168:221–229. https://doi.org/10.1016/S0378-5173(98)00092-1

Fu Q, Sun J, Zhang W et al (2009) Nanoparticle albumin-bound (NAB) technology is a promising method for anti-cancer drug delivery. Recent Pat Anticancer Drug Discov 4:262–272. https://doi.org/10.2174/157489209789206869

Gallo JM, Hung CT, Perrier DG (1984) Analysis of albumin microsphere preparation. Int J Pharm 22:63–74. https://doi.org/10.1016/0378-5173(84)90046-2

Gradishar WJ, Tjulandin S, Davidson N et al (2005) Phase III trial of nanoparticle albumin-bound paclitaxel compared with polyethylated castor oil-based paclitaxel in women with breast cancer. J Clin Oncol 23:7794–7803. https://doi.org/10.1200/jco.2005.04.937

Hechler D, Nitsch R, Hendrix S (2006) Green-fluorescent-protein-expressing mice as models for the study of axonal growth and regeneration in vitro. Brain Res Rev 52:160–169. https://doi.org/10.1016/j.brainresrev.2006.01.005

Italia JL, Bhatt DK, Bhardwaj V et al (2007) PLGA nanoparticles for oral delivery of cyclosporine: nephrotoxicity and pharmacokinetic studies in comparison to Sandimmune Neoral®. J Control Release 119:197–206. https://doi.org/10.1016/j.jconrel.2007.02.004

Jithan A, Madhavi K, Madhavi M, Prabhakar K (2011) Preparation and characterization of albumin nanoparticles encapsulating curcumin intended for the treatment of breast cancer. Int J Pharm Investig 1:119. https://doi.org/10.4103/2230-973X.82432

Kalaria DR, Sharma G, Beniwal V, Ravi Kumar MNV (2009) Design of biodegradable nanoparticles for oral delivery of doxorubicin: in vivo pharmacokinetics and toxicity studies in rats. Pharm Res 26:492–501. https://doi.org/10.1007/s11095-008-9763-4

Karatas H, Aktas Y, Gursoy-ozdemir Y et al (2009) A nanomedicine transports a peptide caspase-3 inhibitor across the blood–brain barrier and provides neuroprotection. J Neurosci 29:13761–13769. https://doi.org/10.1523/jneurosci.4246-09.2009

Kim B, Lee C, Lee ES et al (2016) Paclitaxel and curcumin co-bound albumin nanoparticles having antitumor potential to pancreatic cancer. Asian J Pharm Sci 11:708–714. https://doi.org/10.1016/j.ajps.2016.05.005

Kratz F (2008) Albumin as a drug carrier: design of prodrugs, drug conjugates and nanoparticles. J Control Release 132:171–183. https://doi.org/10.1016/j.jconrel.2008.05.010

Krishna Sailaja A, Vineela C (2014) Preparation and characterization of mefenamic acid loaded bovine serum albumin nanoparticles by desolvation technique using acetone as desolvating agent. Der Pharm Lett 6:207–226. https://doi.org/10.2174/221173850466616 05191

Kulandaivelu K, Mandal AKA (2017) Improved bioavailability and pharmacokinetics of tea polyphenols by encapsulation into gelatin nanoparticles. IET Nanobiotechnol 11:469–476. https://doi.org/10.1049/iet-nbt.2016.0147

Kumar G, Sharma S, Shafiq N et al (2011) Pharmacokinetics and tissue distribution studies of orally administered nanoparticles encapsulated ethionamide used as potential drug delivery system in management of multi-drug resistant tuberculosis. Drug Deliv 18:65–73. https://doi.org/10.3109/10717544.2010.509367

Kumar S, Meena R, Paulraj R (2016) Fabrication of BSA-green tea polyphenols-chitosan nanoparticles and their role in radioprotection: a molecular and biochemical approach. J Agric Food chem 64:6024–6034. https://doi.org/10.1021/acs.jafc.6b02068

Kumari M, Prasad M, Patnaik S, Shukla Y (2018) Curcumin loaded selenium nanoparticles synergize the anticancer potential of doxorubicin contained in self-assembled, cell receptor targeted nanoparticles. Eur J Pharm Biopharm 130:185–199. https://doi.org/10.1016/j.ejpb.2018.06.030

Lambert Joshua D, Yang Chung S (2003) Mechanisms of cancer prevention by tea constituents. J Nutr 133:3244S–3246S. https://doi.org/10.3945/ajcn.113.060186.Am

Lee JH, Shin YC, Yang WJ et al (2014) Epigallocatechin-3-O-gallate-loaded poly(lactic-*co*-glycolic acid) fibrous sheets as anti-adhesion barriers. J Biomed Nanotechnol 11:1461–1471. https://doi.org/10.1166/jbn.2015.2080

Leichsenring A, Bäcker I, Furtmüller PG et al (2016) Long-term effects of (−)-epigallocatechin gallate (EGCG) on pristane-induced arthritis (PIA) in female dark agouti rats. PLoS One 11:1–27. https://doi.org/10.1371/journal.pone.0152518

Li C, Zhang D, Guo Y et al (2014a) Galactosylated bovine serum albumin nanoparticles for parenteral delivery of oridonin: tissue distribution and pharmacokinetic studies. J Microencapsul 31:573–578. https://doi.org/10.3109/02652048.2014.898705

Li Z, Ha J, Zou T, Gu L (2014b) Fabrication of coated bovine serum albumin (BSA)-epigallocatechin gallate (EGCG) nanoparticles and their transport across monolayers of human intestinal epithelial Caco-2 cells. Food Funct 5:1278–1285. https://doi.org/10.1039/c3fo60500k

Lockman PR, Mumper RJ, Khan MA, Allen DD (2002) Nanoparticle technology for drug delivery across the blood–brain barrier. Drug Dev Ind Pharm 28:1–13. https://doi.org/10.1081/DDC-120001481

Merodioa M, Irachea JM, Eclancher F et al (2000) Distribution of albumin nanoparticles in animals induced with the experimental allergic encephalomyelitis. J Drug Target 8:289–303. https://doi.org/10.3109/10611860008997907

Nakagawa K, Okuda S, Miyazawa T (1997) Dose-dependent Incorporation of tea catechins, (−)-epigallocatechin-3-gallate and (−)-epigallocatechin, into human plasma. Biosci Biotechnol Biochem 61:1981–1985. https://doi.org/10.1271/bbb.61.1981

Nayak AP, Tiyaboonchai W, Patankar S et al (2010) Curcuminoids-loaded lipid nanoparticles: novel approach towards malaria treatment. Colloids Surf B Biointerfaces 81:263–273. https://doi.org/10.1016/j.colsurfb.2010.07.020

Pant MP, Mariam J, Joshi A, Dongre PM (2014) ScienceDirect UV radiation sensitivity of bovine serum albumin bound to silver nanoparticles. J Radiat Res Appl Sci 7:399–405. https://doi.org/10.1016/j.jrras.2014.07.004

Patel BK, Parikh RH, Aboti PS (2013) Development of oral sustained release rifampicin loaded chitosan nanoparticles by design of experiment. J Drug Deliv 2013:1–10. https://doi.org/10.1155/2013/370938

Pool H, Quintanar D, Figueroa JDD et al (2012) Antioxidant effects of quercetin and catechin encapsulated into PLGA nanoparticles. J Nanomater. 2012:1–12. https://doi.org/10.1155/2012/145380

Qi C, Chen Y, Jing QZ, Wang XG (2011) Preparation and characterization of catalase-loaded solid lipid nanoparticles protecting enzyme against proteolysis. Int J Mol Sci 12:4282–4293. https://doi.org/10.3390/ijms12074282

Radhakrishnan R, Kulhari H, Pooja D et al (2016) Encapsulation of biophenolic phytochemical EGCG within lipid nanoparticles enhances its stability and cytotoxicity against cancer. Chem Phys Lipids 198:51–60. https://doi.org/10.1016/j.chemphyslip.2016.05.006

Rahmani A, Al Shabrmi FM, Allemailem KS et al (2015) Implications of green tea and its constituents in the prevention of cancer via the modulation of cell signalling pathway. Biomed Res Int 2015:1–8. https://doi.org/10.1155/2015/925640

Ravi TP, Mandal AKA (2015) Effect of alcohol on release of green tea polyphenols from casein nanoparticles and its mathematical modeling. Res J Biotechnol 10:99–104

Rice-Evans CA, Miller NJ, Bolwell PG et al (1995) The relative antioxidant activities of plant-derived polyphenolic flavonoids. Free Radic Res 22:375–383

Saneja A, Nayak D, Srinivas M et al (2017) Development and mechanistic insight into enhanced cytotoxic potential of hyaluronic acid conjugated nanoparticles in CD44 overexpressing cancer cells. Elsevier B.V., Amsterdam

Sanoj Rejinold N, Muthunarayanan M, Chennazhi KP et al (2011) Curcumin loaded fibrinogen nanoparticles for cancer drug delivery. J Biomed Nanotechnol 7:521–534. https://doi.org/10.1166/jbn.2011.1320

Schroeder EK, Kelsey NA, Doyle J et al (2009) Green tea epigallocatechin 3-gallate accumulates in mitochondria and displays a selective antiapoptotic effect against inducers of mitochondrial oxidative stress in neurons. Antioxid Redox Signal 11:469–480. https://doi.org/10.1089/ars.2008.2215

Singh AK, Chakravarty B, Chaudhury K (2015) Nanoparticle-assisted combinatorial therapy for effective treatment of endometriosis. J Biomed Nanotechnol 11:789–804

Singh NA, Bhardwaj V, Ravi C et al (2018a) EGCG nanoparticles attenuate aluminum chloride induced neurobehavioral deficits, beta amyloid and tau pathology in a rat model of Alzheimer's disease. Front Aging Neurosci 10:1–13. https://doi.org/10.3389/fnagi.2018.00244

Singh NA, Kalam A, Mandal A, Khan ZA (2018b) Inhibition of Al(III)-induced Aβ42 fibrillation and reduction of neurotoxicity by epigallocatechin-3-gallate nanoparticles. J Biomed Nanotechnol 14:1147–1158. https://doi.org/10.1166/jbn.2018.2552

Stringer M, Abeysekera I, Thomas J et al (2017) Epigallocatechin-3-gallate (EGCG) consumption in the Ts65Dn model of Down syndrome fails to improve behavioral deficits and is detrimental to skeletal phenotypes. Physiol Behav. https://doi.org/10.1016/j.physbeh.2017.05.003

Suresh G, Manjunath K, Venkateswarlu V, Satyanarayana V (2007) Preparation, characterization, and in vitro and in vivo evaluation of lovastatin solid lipid nanoparticles. AAPS PharmSciTech 8:24. https://doi.org/10.1208/pt0801024

Syame SM, Eisa ZM, Eltayeb R et al (2018) Synthesis and characterization of cisplatin-loaded BSA (bovine serum albumin) nanoparticles as drug delivery system against pancreatic cancer cells. IOSR J Pharm 8:39–48

Tang QS, Chen DZ, Xue WQ et al (2011) Preparation and biodistribution of 188Re-labeled folate conjugated human serum

Springer

albumin magnetic cisplatin nanoparticles (188Re-folate-CDDP/HSA MNPs) in vivo. Int J Nanomed 6:3077–3085. https://doi.org/10.2147/IJN.S24322

Thangapazham RL, Singh AK, Sharma A et al (2007) Green tea polyphenols and its constituent epigallocatechin gallate inhibits proliferation of human breast cancer cells in vitro and in vivo. Cancer Lett 245:232–241. https://doi.org/10.1016/j.canlet.2006.01.027

Tian X, Yang X, Wang K, Yang X (2006) The efflux of flavonoids morin, isorhamnetin-3-*O*-rutinoside and diosmetin-7-*O*-β-D-xylopyranosyl-(1-6)-β-D-glucopyranoside in the human intestinal cell line Caco-2. Pharm Res 23:1721–1728. https://doi.org/10.1007/s11095-006-9030-5

Tominari T, Matsumoto C, Watanabe K et al (2015) Epigallocatechin gallate (EGCG) suppresses lipopolysaccharide-induced inflammatory bone resorption, and protects against alveolar bone loss in mice. FEBS Open Bio 5:522–527. https://doi.org/10.1016/j.fob.2015.06.003

Ulbrich K, Michaelis M, Rothweiler F et al (2011) Interaction of folate-conjugated human serum albumin (HSA) nanoparticles with tumour cells. Int J Pharm 406:128–134. https://doi.org/10.1016/j.ijpharm.2010.12.023

Vivek K, Reddy H, Murthy RSR (2007) Investigations of the effect of the lipid matrix on drug entrapment, in vitro release, and physical stability of olanzapine-loaded solid lipid nanoparticles. AAPS PharmSciTech 8:E83. https://doi.org/10.1208/pt0804083

Weber C, Coester C, Kreuter J, Langer K (2000) Desolvation process and surface characterisation of protein nanoparticles. Int J Pharm 194:91–102. https://doi.org/10.1016/S0378-5173(99)00370-1

Weinreb O, Mandel S, Amit T, Youdim MB (2004) Neurological mechanisms of green tea polyphenols in Alzheimer' s and Parkinson' s diseases. J Nutr Biochem 15:506–516. https://doi.org/10.1016/j.jnutbio.2004.05.002

Woods A, Patel A, Spina D et al (2015) In vivo biocompatibility, clearance, and biodistribution of albumin vehicles for pulmonary drug delivery. J Control Release 210:1–9. https://doi.org/10.1016/j.jconrel.2015.05.269

Yang CS, Chen L, Lee M-J, Balentine D, Kuo MC, Schantz SP (1998) Blood and urine levels of tea catechins after ingestion of different amounts of green tea by human volunteers. Cancer Epidemiol Biomarkers Prev 7:351–354

Yang L, Cui F, Cun D et al (2007) Preparation, characterization and biodistribution of the lactone form of 10-hydroxycamptothecin (HCPT)-loaded bovine serum albumin (BSA) nanoparticles. Int J Pharm 340:163–172. https://doi.org/10.1016/j.ijpharm.2007.03.028

Yedomon B, Fessi H, Charcosset C (2013) Preparation of bovine serum albumin (BSA) nanoparticles by desolvation using a membrane contactor: a new tool for large scale production. Eur J Pharm Biopharm 85:398–405. https://doi.org/10.1016/j.ejpb.2013.06.014

Yu Z, Yu M, Zhang Z et al (2014) Bovine serum albumin nanoparticles as controlled release carrier for local drug delivery to the inner ear. 9:1–7. https://doi.org/10.1186/1556-276X-9-343

Zhang L, Zheng Y, Chow MSS, Zuo Z (2004) Investigation of intestinal absorption and disposition of green tea catechins by Caco-2 monolayer model. Int J Pharm 287:1–12. https://doi.org/10.1016/j.ijpharm.2004.08.020

Zhang H, Huang N, Yang G et al (2017) Bufalin-loaded bovine serum albumin nanoparticles demonstrated improved anti-tumor activity against hepatocellular carcinoma: preparation, characterization, pharmacokinetics and tissue distribution. Oncotarget 8:63311–63323. https://doi.org/10.18632/oncotarget.18800

Zhao D, Zhao X, Zu Y et al (2010) Preparation, characterization, and in vitro targeted delivery of folate-decorated paclitaxel-loaded bovine serum albumin nanoparticles. Int J Nanomed 5:669–677. https://doi.org/10.2147/IJN.S12918